The onset of an electric field-induced ferroelectric-like phase in the perovskite $Pb(Mg_{1/3}Nb_{2/3})O_3$

1996 J. Phys.: Condens. Matter 8 8017

(http://iopscience.iop.org/0953-8984/8/42/020)

J. Phys.: Condens. Matter **8** (1996) 8017–8026. Printed in the UK

The onset of an electric field-induced ferroelectric-like phase in the perovskite $Pb(Mg_{1/3}Nb_{2/3})O_3$

O Bidault†, M Licheron†‡, E Husson†‡ and A Morell§

† LPMM, ESEM, rue Léonard de Vinci, 45072 Orléans Cedex 02, France
‡ CRPHT-CNRS, 45071 Orléans Cedex 02, France
§ Thomson CSF, LCR, Domaine de Corbeville, 91404 Orsay Cedex, France

Received 2 February 1996, in final form 8 July 1996

Abstract. We study the effect of DC electric field application on a $Pb(Mg_{1/3}Nb_{2/3})O_3$ ceramic by impedance spectroscopy and depolarization current measurements. The results indicate the onset of a true ferroelectric phase, characterized by long-range order, instead of a glassy one. The 'freezing' temperature deduced from the Vogel–Fulcher relationship coincides with the phase transition one, whereas the fitted relaxation frequency displays a minimum, as in usual ferroelectrics. The chemical and physical structure of the material is the key parameter to understand the dielectric response which results both from the clusters' dynamics and from their development.

1. Introduction

Lead magnesium niobate, $Pb(Mg_{1/3}Nb_{2/3})O_3$ (PMN), which exhibits a 'diffuse phase transition', is often considered as the prototype of the relaxor ferroelectrics. Within the Curie range (about 270 K), the dielectric permittivity achieves high values and displays a large dispersion [1]. It is now believed that this broad dielectric maximum does not correspond to a phase transition. Indeed, optical and x-ray studies fail to show any structural macroscopic transition: the mean structure remains cubic down to 5 K whereas a macroscopic polarization cannot be observed even for temperatures significantly below the permittivity maximum. Moreover, profile analysis of the x-ray and neutron diffraction lines shows that correlated clusters with $\langle 111 \rangle$ distortions develop upon cooling from about 600 K [2, 3]. On the other hand, high-resolution electron microscopy images [4–6] indicate the presence of ordered regions characterized by a regular one-by-one alternation of the Mg^{2+} and Nb^{5+} cations on the perovskite B sites. These non-stoichiometric (negatively charged) homogeneous regions extending over about 25 Å and occupying approximately a third of the total volume [6] are regularly spread inside a Nb-rich matrix.

On cooling the rhombohedral randomly oriented polar nanodomains, resulting from short-range correlated atomic shifts, progressively nucleate in the matrix due to the strong polarizability of the Nb^{5+} ions. At 5 K, the correlation length of the polar clusters is evaluated to be about 100 Å [3]: their growth seems to be inhibited by the quenched compositional fluctuations and the induced random fields. Thus the polar regions never reach a sufficient degree of development to induce a strong correlation between neighbouring clusters needed for long-range ferroelectric order: the material undergoes a transition from a paraelectric to a non-ergodic low-temperature phase [7]. In this picture, PMN is a

0953-8984/96/428017+10$19.50

highly inhomogeneous material in which cation ordering underlies the relaxor behaviour, establishing a clear link between material structure and physical properties.

Thus the dielectric maximum in the $\epsilon_1(T)$ curve, recorded at a fixed frequency, can be seen as a dynamic effect due to relaxational processes. Indeed, dielectric dispersion demonstrates the occurence of two different relaxation branches [8, 9]. The high-frequency one ($f > 10^7$ Hz) has been reported both in the low- and in the high-temperature regions and ascribed to correlated chains of off-centred Nb cations [8] in analogy to earlier measurements in other perovskites. On the other hand, the low-frequency relaxation slows down regularly and reaches values as low as 10^{-3} Hz in the vicinity of 240 K [10]: no critical behaviour can be observed and the relaxation disappears from the experimental frequency window by slowing down beyond the laboratory time scale [9].

The low-temperature phase has been interpreted as a glassy state [11] characterized by a supposed freezing of polarization fluctuations due to correlations between polar regions. Moreover, the logarithmically broad spectrum of relaxation times, the divergence of the non-linear susceptibility [10] and the appearance of history-dependent effects can be seen as signs of the glassy nature of this phase. On the other hand, ferroelectric long-range ordering can be extended throughout the sample either by introducing Ti^{4+} ions into the B sites [12] or by applying a DC electric field [13] as indicated by x-ray diffraction results. In the first case, transmission electron microscopy studies show that the size of ordered regions is reduced by Ti doping [14], allowing a strong correlation between clusters on cooling. In pure PMN, the external field helps polar clusters to grow and tends to orientate them parallel to the field. As a result, a macroscopic cubic–rhombohedral phase transition occurs in the two cases. This phenomenon can also be detected by dielectric experiments versus temperature under different E field strengths [15]. On cooling and provided E is stronger than a threshold value ($E_{th} = 1.7$ kV cm^{-1} in a crystal [7] or 4 kV cm^{-1} in a ceramic [16]), an additional peak is observed in the $\epsilon(T)$ curves at a field-dependent temperature. The transition from a glassy state to a ferroelectric phase has recently been observed by the time evolution of the dielectric susceptibility when a field is switched on [17]. From such measurements a temperature–field phase diagram delimiting the paraelectric, glassy and ferroelectric phases has been proposed [7, 17].

The aim of the present work is to investigate the appearance of the electric field-induced ferroelectric phase in pure PMN ceramic for different sequences of DC field application during cooling or heating, by means of dielectric measurements and depolarization studies. The extension of the rhombohedral symmetry from Nb-rich clusters up to a macroscopic scale is discussed.

2. Experiment

The $Pb(Mg_{1/3}Nb_{2/3})O_3$ samples were prepared in the form of discs at Thomson-CSF/LCR according to the columbite method, in order to avoid the formation of a pyrochlore phase. The faces were electroded using gold vapour deposition. The dielectric susceptibility measurements were performed with a Schlumberger SI1260 impedance analyser in the frequency range from 1–10^7 Hz. The permittivity was determined by measuring the capacitance and loss tangent as a function of temperature and frequency. The sample temperature could be monitored in the range 77–400 K with an accuracy better than 0.1 K. Moreover, a DC field ($0 \leqslant E \leqslant 10$ kV cm^{-1}) can be applied during measurements. The ceramic pellets were carefully polished so that their thicknesses were in the range 0.2–1 mm. This value was determined by the following two considerations: firstly, the sample has to be kept sufficiently small in order to reach high field strength; secondly, too large a capacitance

yields a resonance in the experimental frequency window.

All the measurements were carried out on samples freshly annealed at a sufficiently high temperature to erase all the effects of previous treatments and especially to eliminate possible remanent polar regions. A preliminary heating and cooling cycle was also necessary to ensure reproductibility. A typical temperature run (rate ± 1 K min^{-1}) was to start from 390 K. The sample was cooled to 77 K under a DC field (field cooling, FC) or under zero field (ZFC). Then, when the low temperature had been reached and before heating, the DC field was maintained (field heating after field cooling, FHFC), or switched off (zero-field heating after field cooling, ZFHFC), or switched on (field heating after zero-field cooling, FHZFC).

The thermal de-poling currents were also measured as a function of temperature in the ZFHFC protocol with a Keithley 617 electrometer. The heating rate was fixed at 2 K min^{-1}. The remanent polarization can then be calculated by integration.

3. Results and discussion

The dielectric response $\epsilon^* = \epsilon_1 - \mathrm{j}\epsilon_2$ of PMN exhibits the well-known relaxor behaviour. A dispersion is observed both in the real and in the imaginary component only around and below the temperature of the dielectric permittivity maximum ($T_{\max}$). This value depends on the measurement frequency, following the empirical Vogel–Fulcher relationship

$$f = f_0 \exp\left[-E_a/\left(T_{\max} - T_f\right)\right] \tag{1}$$

where the pre-exponential factor f_0, the activation energy E_a and the 'freezing temperature' T_f are adjustable parameters.

Analysing the ϵ^* dispersion at fixed temperature or the $\epsilon^*(T)$ curves recorded at different spot frequencies yields equivalent results provided that the material obeys a Debye-like characteristic. As recalled in section 1, the occurence in PMN of a superposition of two different dielectric mechanisms arising from the presence of more than one process with overlapping activity in frequency leads to an intricate dielectric response. Thus the Vogel–Fulcher relationship, which is very sensitive to the choice of the data, will be restricted to the 10^2–10^6 Hz range. In this frequency window, the dispersion may be regarded as being primarily associated with the relaxor properties. The high-frequency relaxation, observed in many other perovskites like the normal ferroelectric $BaTiO_3$ [18], does not significantly influence the fitting parameters. A good fit is obtained (not shown here) with $f_0 = 1.68 \times 10^{12}$ Hz, $E_a = 72.3$ meV and $T_f = 227$ K. All these values have the same order of magnitude as those reported for a PMN single crystal [19].

We now turn to a brief description of the dielectric response $\epsilon^*(T)$ recorded for the different cycles: FCFH, FCZFH and ZFCFH. The more interesting curves are reported in figure 1 for a measuring frequency of 10 Hz and an applied electric field of 7.5 kV cm^{-1}. The application of a DC field gives rise to some additional peculiarities in the low-temperature range which are connected to the onset of a macroscopic rhombohedral phase as indicated by x-ray diffraction [13, 20]. Indeed, the shoulder observed on both $\epsilon_1(T)$ and $\epsilon_2(T)$ at T_{pc} in the FC regime provided that $E \geqslant 4$ kV cm^{-1} (curve 3) is due to the phase transition from a relaxor to a ferroelectric phase, as clearly demonstrated by Ye and Schmid for a single crystal [15] (see inset). Indeed, the frequency-independent T_{pc} value (the temperature of poling on cooling) is difficult to determine accurately from measurements performed on a ceramic. The major trend is a weak variation with the field strength from about 200 ($E = 6$ kV cm^{-1}) to about 225 K for $E = 7.5$ and 9 kV cm^{-1}.

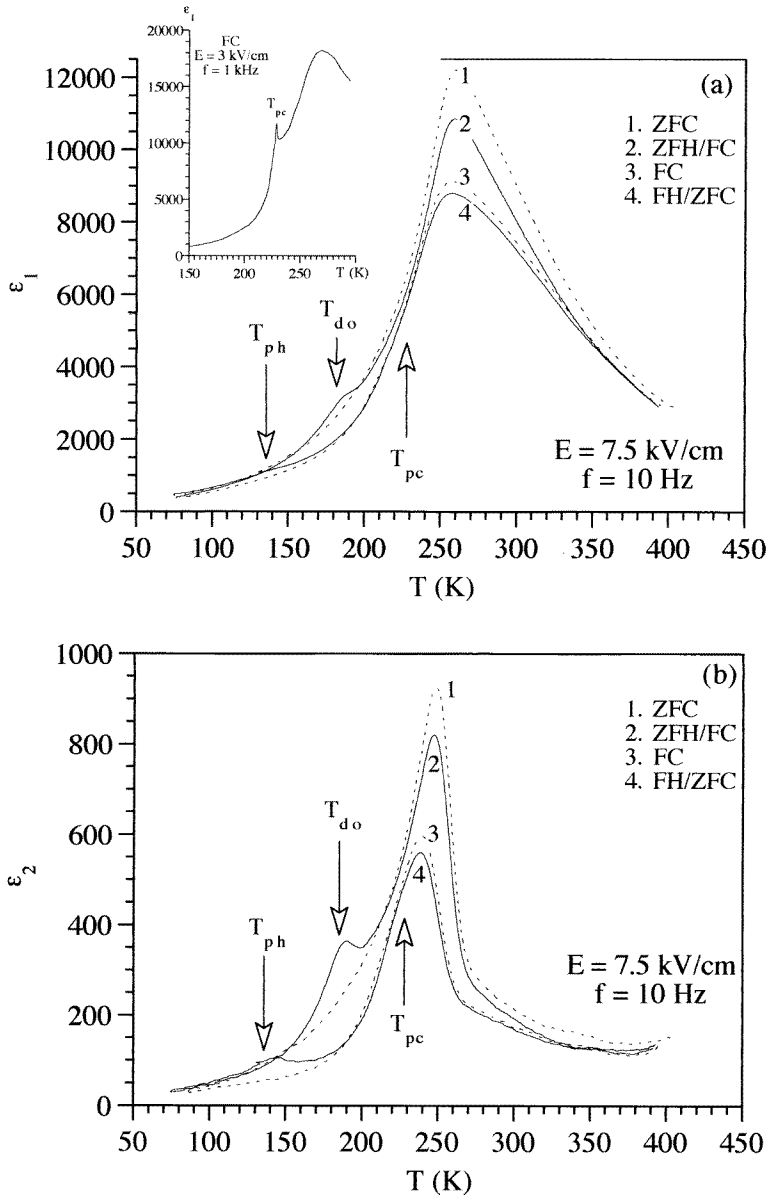

Figure 1. Real (a) and imaginary (b) parts of the dielectric constant recorded at 10 Hz for different DC field sequences: ZFC, ZFHFC, FC and FHZFC. These protocols allow one to define the three temperatures T_{pc}, T_{do} and T_{ph} (shown by the arrows) linked to the onset or disappearance of a ferroelectric macroscopic phase (see the text). Inset: the real part of ϵ^* of a $\langle 111 \rangle$-oriented single crystal measured during cooling under 3 kV cm^{-1} (FC, $f = 1$ kHz): the anomaly at T_{pc} is clearer than it would be in a ceramic. Data from Ye and Schmid [15].

At 77 K, if the field is switched off and the temperature swept up again (ZFHFC: curve 2), a new anomaly is clearly detected at a temperature of 185 K, called T_{do} (the

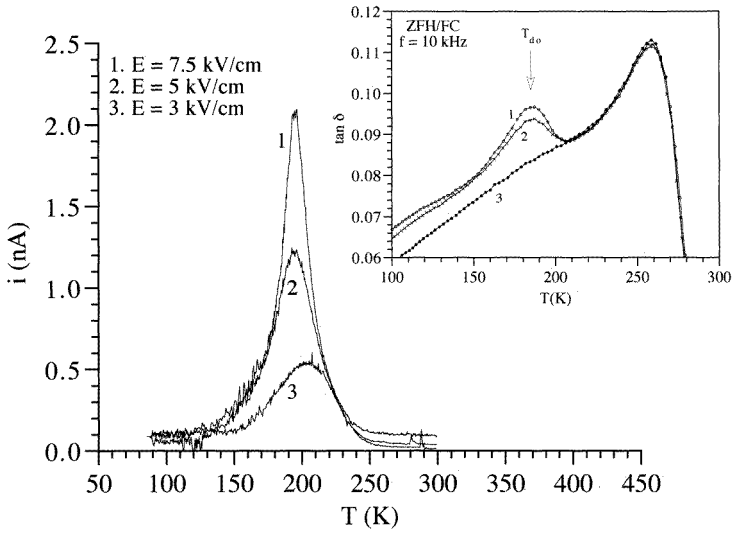

Figure 2. Depolarization currents and dielectric losses (inset) measured during ZFH after FC runs under different field strengths: 1, $E = 7.5$; 2, $E = 5$ and 3, $E = 3$ kV cm^{-1}.

temperature of de-poling under 0 kV cm^{-1}), independently of the initial poling field strength. It can be seen as proof of the field-free de-polarization. On the other hand, if the field is maintained during the heating (the FHFC regime, not shown on figure 1), the de-poling takes place at a temperature higher than T_{do} and quite similar to the T_{pc} value observed on cooling. A third temperature can be defined: T_{ph} (the temperature of poling on heating). Indeed, heating under a great enough DC field a zero-field cooled sample (FHZFC: curve 4) induces a poling process. The ferroelectric phase appears at a temperature, T_{ph}, depending on the applied field amplitude: when E is lowered to the threshold value, T_{ph} increases and finally vanishes near T_{pc} as in the FHFC cycle.

It is worthwhile to note that the temperatures T_{pc}, T_{do} and T_{ph} are insensitive to the measuring frequency, unlike the dispersive behaviour of the broad maximum, even under bias field. All these observations are qualitatively in good agreement with the results obtained on single crystals [7, 15]. In summary, the application of a DC field gives rise to the build-up of a macroscopic polar phase by the growth and ordering of the polar microregions which develop on cooling in the relaxor state: the non-ergodic low-temperature phase exhibiting glass-like properties disappears for cooling fields stronger than 4 kV cm^{-1} in favour of a ferroelectric one.

The disappearance during a ZFHFC of the low-temperature field-induced phase has also been investigated by de-poling current measurements for poling field strengths in the range 0–7.5 kV cm^{-1}. The temperature dependence of the measured current is shown in figure 2 for different E values, lower than the threshold (3 kV cm^{-1}) or higher (5 and 7.5 kV cm^{-1}). A broad maximum is detected in all cases, even for $E \leqslant E_{th}$. Its amplitude decreases regularly as the applied poling field decreases to 0 kV cm^{-1}. The remanent polarization at 100 K, calculated by integrating the $i(T)$ curves, varies linearly with E up to 31.4 μC cm^{-2} for $E = 7.5$ kV cm^{-1}. No plateau value is reached and no jump can be observed in the $P_r(E)$ curve at and below the threshold field. A similar effect has been reported in a crystal for a field applied along the ⟨100⟩ direction [7]. For $E \geqslant E_{th}$, a rather

wide de-poling peak extending over about 100° is detected, reaching a maximum at nearly 195 K. This observation is consistent with the dielectric data (see inset) characterized by a discontinuity at T_{do} ($\approx$ 185 K), independently of the initial poling strength which only controls the anomaly amplitude. We have already recalled that the application of a DC field below 4 kV cm^{-1}, be it during cooling or heating, does not create anomalies in the dielectric constant, at least in the investigated frequency range ($f \geqslant 10$ Hz). A rounded maximum, instead of a peak, is clearly seen by measuring the pyroelectric current. By cooling the sample under such low fields, a metastable polarization is created as judged from isothermal depolarization measurements indicating a regular polarization decrease versus time [7]. In each grain of the ceramic, the DC electric field induces the growth and the gradual alignment of the polar clusters along one of the ⟨111⟩ directions favoured by the field application. At the threshold value, the transition is changed from a glass-like to a structural one with ferroelectric domains of rhombohedral symmetry.

We now turn to the effect of the field-induced phase transition on the dielectric dispersion. PMN is known to exhibit a complex dielectric response. Without any applied DC field, as recalled in section 1, two different relaxations have been reported [8]. The authors of this earlier study have shown that the response function of the complex permittivity can be fitted in the frequency interval 10^2–10^9 Hz using a Cole–Cole model for each relaxation. In the following, we take into account only the low-frequency one ($f \leqslant 10^7$ Hz), characteristic of a relaxor material. It is only detected below $T_{\max}$ and seems to slow down regularly as the temperature decreases.

Other models were also employed to analyse the dielectric dispersion data, like that based on Ngai's theory [21]. Moreover, based on low-frequency ($3 \times 10^{-3} \leqslant f \leqslant 10^2$ Hz) measurements [10], fits were recently performed with the Havriliak–Negami expression [9]. In all cases, the deduced fitting parameters change with temperature, but no extremum is found: the relaxation frequency in PMN does not reach a minimum at a transition temperature, in contrast to the case of ferroelectrics, but disappears completely from the experimental window (see figure 4, curve for 0 kV cm^{-1}). Up to now, to our knowledge, dispersion curves $\epsilon^*(\omega)$ recorded during field application have never been published and the effect of the onset of the ferroelectric phase upon the relaxation frequency never described.

In the present study, dielectric measurements were performed covering seven frequency decades (10^0–10^7 Hz), as the sample is cooled without any applied field or under 3, 5, 6, 7.5 and 9 kV cm^{-1}. In the four last cases, the field strength is high enough to induce a ferroelectric phase transition. Several disc-shaped samples with different geometrical parameters were also tested with no detectable effect. As a representative example of the obtained results, figure 3 depicts the frequency dependences both of ϵ_1 and of ϵ_2 under $E = 6$ kV cm^{-1}. The curve shape can be interpreted in terms of a Debye-like behaviour. Indeed, the dielectric response can still be fitted using the Cole–Cole equation, as earlier shown during a field-free cooling [8]:

$$\epsilon^*(\omega) = \epsilon_1(\omega) - \mathrm{j}\epsilon_2(\omega) = \epsilon_\infty + \frac{\epsilon_s - \epsilon_\infty}{1 + (\mathrm{j}\omega\tau)^{(1-\alpha)}} \tag{2}$$

where ϵ_∞ is the high-frequency value of the dielectric susceptibility and ϵ_s its low-frequency limit. The parameter α is used to fit the relaxation broadening around the most probable relaxation time τ. The fittings were mainly attempted on the real part of the dielectric susceptibility $\epsilon_1(\omega)$. Indeed, calculation on $\epsilon_2(\omega)$ was sometimes not efficient enough due to unwanted effects, like conductivity at low frequencies ($f < 100$ Hz) because of field application, or extrinsic set-up resonance, which affects measurements for frequencies higher than 10^5 Hz due to the sample thickness. The fact that ϵ_1 is less sensititive to these

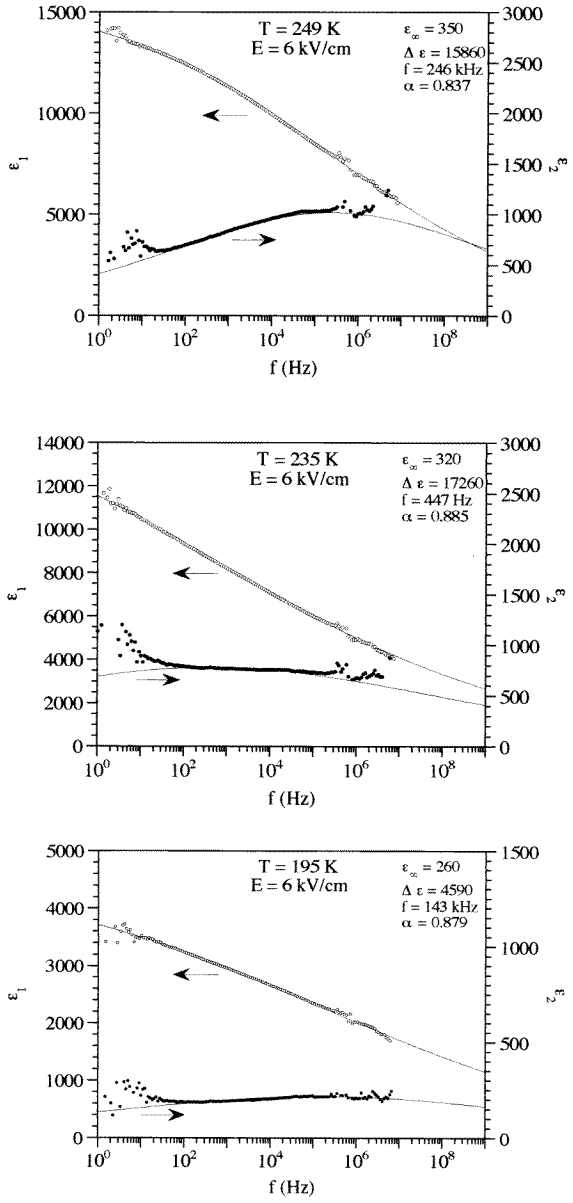

Figure 3. The frequency dependence of the real and imaginary parts of the dielectric susceptibility recorded under 6 kV cm^{-1} at different temperatures. Circles are experimental points and lines are best fits using equation (2). The fitting parameters are given for each plot.

contributions allows the relaxational parameters to be evaluated with some precision by overcoming the perturbations. As shown in figure 3, the good fit between experimental points and theoretical curves for a dipolar relaxation of Cole–Cole type is clear.

The relaxation parameters have been determined at different temperatures for different field strengths. As an example, the values deduced from equation (2) are reported in figure 3

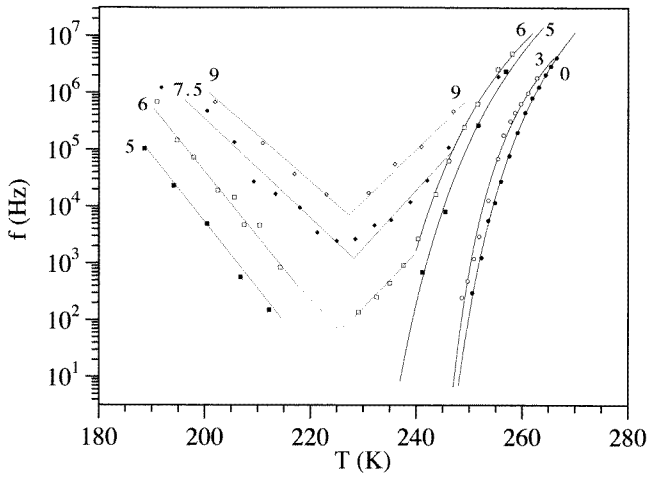

Figure 4. Relaxation amplitude as a function of temperature. The number indicates the field strength applied on the sample during cooling.

for 6 kV cm^{-1} at 249, 235 and 195 K. It is clear from such plots that a critical effect takes place in this temperature range. Although the samples of interest are of diverse shapes and the dielectric constant changes smoothly with temperature without displaying any extremum, we stress that this effect cannot be ascribed to an extrinsic contribution.

For each case ($0 \leqslant E \leqslant 9$ kV cm^{-1}), the α values, corresponding to the relaxation time distribution, are very large (0.7–0.9) and increase regularly when the temperature decreases down to about 230 K, a temperature at which α hardly changes any longer. On the other hand, the field induces only a weak change of a few per cent: for each field strength, the $\alpha(T)$ variation remains close to the one described earlier for a zero-field-cooling protocol [8]. The ϵ_∞ parameter, which in practice corresponds to the permittivity measured above the dispersion region, is difficult to determine accurately. Indeed, in our frequency window, no constant value is reached even at 10^7 Hz, due to the large distribution of relaxation times (see the dispersion curves $\epsilon_1(\omega)$, figure 3). Fits lead to low ϵ_∞ values decreasing as temperature decreases or field strength increases. The dispersion step $\Delta\epsilon = \epsilon_s - \epsilon_\infty$ decreases more and more as the field strength is raised. The $\Delta\epsilon(T)$ curve shape changes continuously and exhibits an extremum for $E \geqslant E_{th}$ (for example $E = 7.5$ kV cm^{-1}). In fact, among the fitting parameters, the most field dependent is $f = (1/2\pi\tau)$, the relaxation frequency. At about 250 K and for $E = 0$ kV cm^{-1}, we get $f = 1$ kHz. This value shifts over three orders of magnitude up to about 4.7×10^5 Hz for $E = 9$ kV cm^{-1} as the field strength is raised. The most interesting result is the variation of frequency with temperature which will be discussed now.

All the fitted f values are reported on a logarithmic scale as a function of temperature in figure 4. For the field-free experiment, the relaxation frequency slows down regularly as expected, following a Vogel–Fulcher behaviour with an adjustable T_f temperature of 228 K. This value is very close to the one found previously from the measurements recorded at fixed frequencies during cooling (227 K). The same behaviour can be observed for $E = 3$ kV cm^{-1}. It is worth pointing out that the frequency variation upon varying the temperature is quite different when a field stronger than the threshold value is applied. In particular, a minimum value is reached in the vicinity of 225–230 K whereas the $f(T)$

curves are approximately straight lines below 240 K (on a semi-logarithmic scale). For 7.5 and 9 kV cm^{-1}, fields for which f stays within our experimental frequency window, the minimum occurs in both cases at about 228 K. This is typical of ferroelectric phase transitions. It is worthwhile to note that this critical temperature, T_c, is quite similar to the 'freezing' one, T_f, and also to the T_{pc} value. Thus, by determining the characteristic frequency of the relaxor PMN and provided the field strength is higher than the threshold value, we demonstrate the occurrence of criticality in the vicinity of the phase transition temperature. The maximum dielectric response, the minimum relaxation frequency and the onset of a macroscopic electric polarization all occur at the same temperature.

Two remarks have to be made. Firstly, in the phase transition region, the relaxation frequency does not behave like $f \propto |T - T_c|$, as predicted for an order–disorder transition in a material containing permanent dipoles. It rather follows an exponential law, $f \propto \exp|T - T_c|$. We have no specific explanation for such an observation. Bearing in mind the temperature dependence of the size of the polar clusters, a more complex picture is probably needed. Secondly, the coincidence between the ferroelectric phase transition temperature and the T_f value has already been noted in several materials, like $Pb(Mg_{1/3}Nb_{2/3})O_3$–10% Ti [12] and the disordered stoichiometric $Pb(Sc_{1/2}Ta_{1/2})O_3$ [22] and $Pb(Sc_{1/2}Nb_{1/2})O_3$ [23] ceramics. In these compounds, the transition between the relaxor state into a normal ferroelectric phase is no longer field-induced: by controlling the chemical structure (Ti doping in one case, lead vacancies in the others), the material is made to undergo a spontaneous transition. In all these cases, neither the transition nor the field application affect the validation of the Vogel–Fulcher relationship in the relaxor state, which leads to a 'freezing' temperature always close to the phase transition one.

When cooling a field-free PMN, the dipoles (polar clusters) dynamics slows down regularly until a supposed freezing takes place at T_f due to the development of correlations between moments, leading to a glassy state [11]. Upon applying a sufficiently high field (or introducing at least 10% Ti), a macroscopic rhombohedral phase appears at a temperature which is found to coincide with T_f. This ferroelectric phase is characterized by long-range order, as indicated by x-ray diffraction [13, 20], whereas its symmetry reflects the local one of the polar clusters. Meanwhile, the physical meaning of the T_f temperature can still be questioned. Indeed, Tagantsev [24] showed recently that the Vogel–Fulcher relationship does not necessarily imply a freezing process. However, its coincidence with the ferroelectric phase transition temperature seems to be a general feature in relaxors.

4. Conclusion

The dielectric and de-poling current measurements performed on a PMN ceramic under DC field indicate the possible onset of a ferroelectric phase. The minimum field strength necessary to induce the macrodomain state is found to be greater than that used in a crystal. Moreover, the field-induced transition occurs in the vicinity of the 'freezing' temperature, T_f. At the same time, by fitting the $\epsilon_1(\omega)$ curves recorded under field with the Cole–Cole equation, an extremum is demonstrated for the first time in the temperature dependence of the relaxation parameters. The PMN dielectric response reflects dynamical effects: without any applied field, the relaxation frequency follows the Vogel–Fulcher law connected to the thermal slowing of the dipoles. On the other hand, the field application results in the growth and the gradual alignment of the polar clusters so that long-range ordering takes place, implying a true ferroelectric phase transition.

Acknowledgments

The authors wish to thank Dr M Maglione for valuable discussions.

References

[1] Smolenskii G A, Isupov V A, Agranovskaya A I and Popov S N 1960 *Fiz. Tverd. Tela* **2** 2906 (1960 *Sov. Phys. Solid State* **2** 2584)
[2] Bonneau P, Garnier P, Calvarin G, Husson E, Gavarri J R, Hewat A W and Morell A 1991 *J. Solid State Chem.* **91** 350
[3] de Mathan N, Husson E, Calvarin G, Gavarri J R, Hewat A W and Morell A 1991 *J. Phys.: Condens. Matter* **3** 8159
[4] Husson E, Chubb M and Morell A 1989 *Mater. Res. Bull.* **23** 357
[5] Chen J, Chan H M and Harmer M P 1989 *J. Am. Ceram. Soc.* **72** 593
[6] Boulesteix C, Varnier F, Llebaria A and Husson E 1994 *J. Solid State Chem.* **108** 141
[7] Sommer R, Yushin N K and van der Klink J J 1993 *Phys. Rev.* B **48** 13 230
[8] Elissalde C, Ravez J and Gaucher P 1993 *Mater. Sci. Eng.* B **20** 318
[9] Christen H-M, Sommer R, Yushin N K and van der Klink J J 1994 *J. Phys.: Condens. Matter* **6** 2631
[10] Colla E V, Koroleva E Yu, Okuneva N M and Vakhrushev S B 1992 *J. Phys.: Condens. Matter* **4** 3671
[11] Viehland D, Jang S J, Cross L E and Wuttig M 1992 *Phys. Rev.* B **46** 8003
[12] Bidault O, Licheron M, Husson E, Calvarin G and Morell A 1996 *Solid State Commun.* **98** 765
[13] Arndt H, Sauerbier F, Schmidt G and Shebakov L A 1988 *Ferroelectrics* **79** 145
[14] Randall C A and Bhalla A S 1990 *Japan. J. Appl. Phys.* **29** 327
[15] Ye Z G and Schmid H 1993 *Ferroelectrics* **145** 83
[16] Chabin M, Malki M, Husson E and Morell A 1994 *J. Physique* III **4** 1151
[17] Colla E V, Koroleva E Yu, Okuneva N M and Vakhrushev S B 1995 *Phys. Rev. Lett.* **74** 1681
[18] Kazaoui S, Ravez J, Maglione M and Goux P 1992 *Ferroelectrics* **126** 203
[19] Viehland D, Wuttig M and Cross L E 1991 *Ferroelectrics* **120** 71
[20] Calvarin G, Husson E and Ye Z G 1995 *Ferroelectrics* **165** 349
[21] Tsurumi T, Soejima K, Kamiya T and Daimon M 1994 *Japan. J. Appl. Phys.* **33** 1959
[22] Chu F, Setter N and Tagantsev A K 1993 *J. Appl. Phys.* **74** 5129
[23] Chu F, Reaney I M and Setter N 1995 *J. Appl. Phys.* **77** 1671
[24] Tagantsev A K 1994 *Phys. Rev. Lett.* **72** 1100